

Microsecond-Resolved Infrared Spectroscopy on Nonrepetitive Protein Reactions by Applying Caged Compounds and Quantum Cascade Laser Frequency Combs

Mohamad Javad Norahan, Raphael Horvath, Nathalie Woitzik, Pierre Jouy, Florian Eigenmann, Klaus Gerwert, and Carsten Kötting*



Cite This: *Anal. Chem.* 2021, 93, 6779–6783



Read Online

ACCESS |



Metrics & More

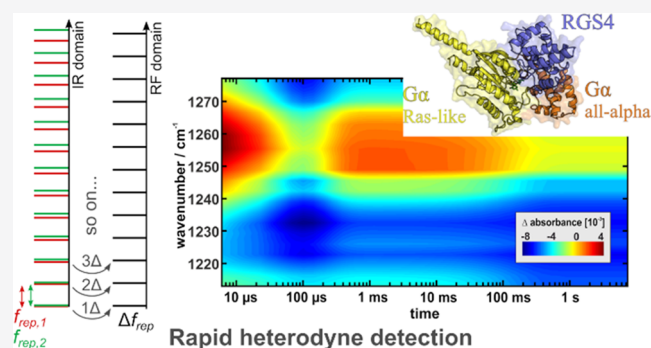


Article Recommendations



Supporting Information

ABSTRACT: Infrared spectroscopy is ideally suited for the investigation of protein reactions at the atomic level. Many systems were investigated successfully by applying Fourier transform infrared (FTIR) spectroscopy. While rapid-scan FTIR spectroscopy is limited by time resolution (about 10 ms with 16 cm^{-1} resolution), step-scan FTIR spectroscopy reaches a time resolution of about 10 ns but is limited to cyclic reactions that can be repeated hundreds of times under identical conditions. Consequently, FTIR with high time resolution was only possible with photoactivable proteins that undergo a photocycle. The huge number of nonrepetitive reactions, e.g., induced by caged compounds, were limited to the millisecond time domain. The advent of dual-comb quantum cascade laser now allows for a rapid reaction monitoring in the microsecond time domain. Here, we investigate the potential to apply such an instrument to the huge class of G-proteins. We compare caged-compound-induced reactions monitored by FTIR and dual-comb spectroscopy by applying the new technique to the α subunit of the inhibiting G_i protein and to the larger protein–protein complex of $G\alpha_i$ with its cognate regulator of G-protein signaling (RGS). We observe good data quality with a $4\text{ }\mu\text{s}$ time resolution with a wavelength resolution comparable to FTIR. This is more than three orders of magnitude faster than any FTIR measurement on G-proteins in the literature. This study paves the way for infrared spectroscopic studies in the so far unresolvable microsecond time regime for nonrepetitive biological systems including all GTPases and ATPases.



INTRODUCTION

Fourier transform infrared (FTIR) spectrometers revolutionized infrared spectroscopy in the 1970s.¹ Likely, the advent of stable mid-IR quantum cascade lasers (QCLs) will impact infrared spectroscopy to the same extent. Conventional QCLs are superior with regard to brilliance,² but they lack the multiplex advantage of FTIR that is especially helpful in time-resolved measurements of proteins. For systems that can be excited repetitively, step-scan FTIR can provide time-resolved spectra with nanosecond resolution.³ For these repetitive systems, tunable QCLs provide time-resolved spectra with 10 ns resolution.^{2,4} Pump-probe experiments (visible pump and IR probe) even allow for femtosecond time-resolved IR spectroscopy.⁵ However, samples that allow only single excitations can either be measured only at a single wavelength⁶ or with rapid-scan FTIR.⁷ The time resolution of rapid-scan FTIR depends on the scanning velocity of the Michelson interferometer and is limited to about 10 ms at a wavelength resolution of 16 cm^{-1} within high-end research FTIR instruments. The implementation of a faster Michelson interferometer allows, in principle, for a higher time resolution,

but with a conventional global as the light source, signal-to-noise ratios (S/N) are not sufficient for single-shot experiments on biological systems.⁸ Synchrotron irradiation in combination with a dispersive setup and an array detector permits single-shot experiments with microsecond resolution.⁹ However, even here S/N was not sufficient for single-shot experiments of a protein reaction.¹⁰

The recent development of dual-comb QCL-based spectrometers allows for microsecond time resolution as well, but with a much smaller footprint.^{11,12} In these instruments, two broad band lasers that emit at many discrete wavelengths are used as the light source (Figure 1). The wavelength spacing of the first laser ($f_{\text{rep},1}$) is close but not identical to the other laser

Received: February 11, 2021

Accepted: April 8, 2021

Published: April 21, 2021



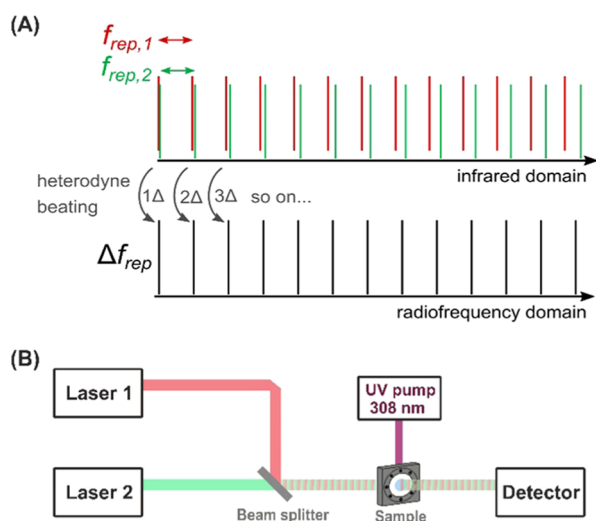


Figure 1. (A) Principle of dual-comb spectroscopy. (B) Schematic of the setup of the dual-comb spectrometer used here.

($f_{\text{rep},2}$). Overlaying the two lasers produces a set of beatings spaced by $\Delta f_{\text{rep}} = f_{\text{rep},1} - f_{\text{rep},2}$ in the radiofrequency domain measured by a high-bandwidth mercury–cadmium–telluride (MCT) detector. From this measurement, the entire heterodyne beating pattern can be recovered. In our setup, Δf_{rep} leads to a time resolution of 4 μs . The spectral window of the lasers is from 1207.0 to 1276.8 cm^{-1} . By guiding the QCLs through a sample that is irradiated by a pulsed UV laser, UV light-induced spectral changes of the sample can be obtained with a time resolution of 4 μs .¹¹

Caged compounds¹³ are a tool for the investigation of reactions of biological systems that can otherwise not be initiated by light. Caged compounds release the reactive compound upon irradiation and cannot be excited repetitively. Rapid-scan FTIR spectrometers usually have a time resolution of about 10 ms at a 16 cm^{-1} spectral resolution. Due to limited S/N, the actual time resolution for measuring protein reactions is often even slower and often artificial low temperatures are necessary to slow down the reaction. Most prominently, ATPases¹⁴ and GTPases¹⁵ were investigated in detail by means of caged nucleotides. As caged compounds, the P³-[1-(2-nitrophenyl)ethyl] ester (NPE)¹⁶ and the P³-[para-hydroxyphenacyl] ester (pHP)¹⁷ of the nucleotides were used.

Here, we used, for the first time, a dual-comb QCL-based spectrometer for the investigation of GTPases in the microsecond time domain. First, we measured the photolysis reaction of two caged GTPs, NPE-GTP¹⁶ and pHP-GTP,¹⁸ in solution without a protein present and compare the results with conventional rapid-scan FTIR. In the next step, we applied the technique to the α subunit of the heterotrimeric G_i protein and monitor its GTPase reaction.¹⁹ Finally, the regulator of G-protein signaling (RGS)-catalyzed reaction of $G\alpha_i$ was measured for the first time at ambient temperatures by time-resolved infrared spectroscopy. At room temperature, the reaction is completed before the first datapoint of a rapid-scan FTIR measurement can be recorded. With dual-comb IR, it is well resolved, including a so far unknown intermediate.

EXPERIMENTAL SECTION

The P³-[1-(2-nitrophenyl)ethyl] ester (NPE) of GTP was obtained from Jena Bioscience (Jena, Germany). The P³-[para-hydroxyphenacyl] ester (pHP) of GTP was synthesized by

coupling GDP with pHP-caged P_i. pHP-P_i was obtained in five steps from para-hydroxy-acetophenone and dibenzylphosphate.¹⁷

$G\alpha_{i1}$ and RGS proteins were expressed and purified as described by Mann et al.¹⁹ In the purified proteins, the nucleotide GDP was exchanged for pHP-GTP. The exchange rate was >95% as checked by reversed-phase high-performance liquid chromatography (HPLC; LC-2010; Shimadzu) [mobile phase: 50 mM Pi (pH 6.5), 5 mM tetrabutylammonium-bromide, 7.5% (vol/vol) acetonitrile; stationary phase: ODS-Hypersil C18 column]. For the intrinsic $G\alpha_{i1}$ measurements, $G\alpha_{i1}$ -pHP-GTP was lyophilized. For the samples, lyophilized protein was resuspended in buffer to reach the following concentrations: 5 mM $G\alpha_{i1}$, 200 mM *N*-(2-hydroxyethyl)-piperazine-*N'*-ethanesulfonic acid (Hepes; pH 7.5), 150 mM NaCl, 5 mM MgCl₂, 200 mM dithiothreitol (DTT), and 0.1% (vol/vol) ethylene glycol. For the RGS-catalyzed reactions, a 1:1 molar ratio of $G\alpha_{i1}$ with RGS was lyophilized and resuspended to reach 5 mM $G\alpha_{i1}$ -RGS, 100 mM Hepes (pH 7.5), 100 mM Tris (pH 7.5), 150 mM NaCl, 5 mM MgCl₂, 20 mM DTT, and 0.1% (vol/vol) ethylene glycol. The samples were packed between two CaF₂ windows, separated by a spacer ring yielding a pathlength of about 60 μm , that were sealed with silicon grease and mounted either in a Bruker Vertex 80v spectrometer or an IRsweep IRis-F1 dual-comb spectrometer. All measurements were done at room temperature (293 K). The reactions were initiated by flashes of a XeCl-excimer laser (308 nm, 150 mJ, Coherent LPX Pro 240). FTIR measurements were recorded at a 4 cm^{-1} spectral resolution, manipulated by zero filling by a factor of 2, and Fourier-transformed using Mertz phase correction and with a Blackman–Harris three-term apodization function.

The operating principles of the IRis-F1 spectrometer have been described in detail.^{11,12,20} Briefly, two continuous-wave QCL frequency combs with $\Delta f_{\text{rep}} = 3.2$ MHz were used to obtain the heterodyne beating signal. Under the operating conditions used here, $f_{\text{rep},1}$ and $f_{\text{rep},2}$ were about 9.82 GHz, as determined from the interline beating measured with a spectrum analyzer (FSW26, Rohde & Schwarz). This gives a native spectral resolution of 0.3275 cm^{-1} . The spectral output of the individual lasers is presented in Figure S1. The power at the sample was adjusted to be about 3 mW. We obtained data in two measurement modes, as described further in Figure S2. In time-resolved mode, each acquisition is 33.6 ms long, sampled at 2 GS/s, and fast Fourier transforms are taken at intervals of 4 μs , which determines the time resolution of the measurement. Time resolutions up to $\frac{1}{\Delta f_{\text{rep}}}$ are possible,^{11,21} but

given the rates of the processes investigated here, and a drop in signal-to-noise ratio at lower integration times, 4 μs was chosen. In this mode, each additional acquisition takes a relatively long time to complete and serves only to improve the signal-to-noise ratio by synchronizing with repeated excitations. In the long-term acquisition mode, each acquisition is 1 ms long and repeats with a frequency of approximately 100 Hz. The time-resolved dual-comb IR data were obtained from combining measurements from both modes, which were each logarithmically averaged. Before merging, the data were scaled according to the difference spectra at peaks wavenumber of each dataset. Furthermore, to avoid discontinuities, we allowed for an ~ 15 ms overlap between both datasets. The originally recorded high spectral resolution of the IRsweep instrument at 0.3275 cm^{-1} was also averaged to 4.2 cm^{-1} for better S/N.

The data were further analyzed by a global fit (eq 1).¹⁵ The time-resolved absorbance change $\Delta A(\nu, t)$ is described by the absorbance change induced by photolysis $a_{\text{ph}}(\nu)$ followed by a number n of exponential functions fitting the amplitudes a for each wavenumber ν . The amplitude spectra have negative peaks for absorptions that disappear (or lose intensity) and positive peaks for absorptions that emerge (or gain intensity).

$$\Delta A(\nu, t) = a_{\text{ph}}(\nu) + \sum_{l=1}^n a_l(\nu)(1 - e^{-k_l t}) \quad (1)$$

For easier comparison, we give the half-life ($t_{1/2} = \ln(2)/k$) in the manuscript. Due to the limited intensity of the excitation beam and the insufficient overlap of the excitation laser with the absorption spectrum of the caged compounds, not the complete sample is photolyzed by one laser flash. Note that a more intense excitation beam could also lead to an increased heat artifact. To estimate the amount of photolysis, the signal strength at the most intense analyte peak (1253 cm^{-1}) was integrated over the first 2 ms after excitation as a function of sample excitation number. This was repeated for the negative times (-2 to 0 ms) as a control, as no spectral features are expected there. Figure S3 indicates that for NPE-GTP after 20 excitations, no further photolysis occurs. For pHP-GTP after 10–15 excitations, no further photolysis is observed (Figure S4), and the data shown are the averages of the first 10 excitations. In the figures of the main text, we always show the results of measurements obtained by a single sample.

RESULTS AND DISCUSSION

Photolysis of NPE-GTP does not produce GTP directly; first, an intermediate aci-nitro anion is formed (Figure 2A).²² Depending on the reaction conditions, GTP is formed from this intermediate, usually in the millisecond time regime. We measured NPE-GTP photolysis with both a Bruker Vertex 80v FTIR spectrometer and an IRsweep IRis-F1 dual-comb spectrometer (Figure 2).

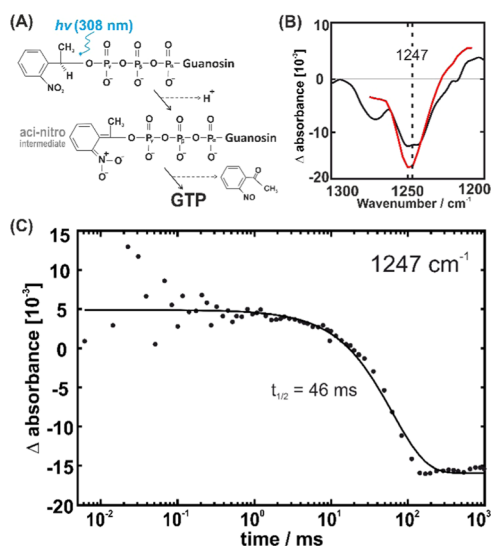


Figure 2. (A) Photolysis of the NPE-GTP reaction scheme. (B) Photolysis spectra obtained by FTIR (black) and dual-comb (red) obtained by global fits of the time-resolved data, respectively. (C) Kinetics of the hydrolysis reaction obtained by dual-comb experiments. The points correspond to the time-resolved data, and the line corresponds to the global fit according to eq 1.

The photolysis difference spectrum of the FTIR experiment can be compared with the same difference from the dual-comb experiment. In both cases, the spectra are shown in a way that the newly formed absorptions are facing upward and vanishing absorptions are facing downward. Figure 2B shows that the spectra agree nicely. The spectral window of the dual-comb experiment shows nicely the vanishing band of the combined asymmetric stretching vibrations of the phosphate groups of the aci-nitro-GTP intermediate.²³

The same reaction was investigated before by a step-scan FTIR experiment with a $10 \mu\text{s}$ time resolution at a spectral resolution of 15 cm^{-1} .²⁴ The data were obtained within 5 h of measurement time, using $200 \times 200 \mu\text{m}^2$ segments from five samples of 1 cm^2 area.²⁵ In comparison, the dual-comb experiment was done with a single sample. Compared to the 5 h of the step-scan FTIR experiment, the dual-comb measurement only took a few seconds. Further, much smaller amounts of sample are needed. The saving in sample consumption is about a factor of 10 in our experiment, but could be improved by another factor of 10 using a cuvette optimized for the QCL profile. The diameter of the laser beam is about 3 mm and much smaller than the conventional IR cuvettes, as shown in Figure S5. The quantum yield of the NPE-GTP hydrolysis with our 308 nm XeCl-excimer laser is limited. For this reason, we repeated the experiment 20 times with the same sample in the same position and co-added the observed changes. The sample response after each shot was monitored (Figure S3). The kinetics in Figure 2B were obtained by combining the time-resolved and long-term measurement modes of the IRis-F1 (details of the data treatment are given in the Experimental Section). We measured a half-life of 46 ms at 293 K for the intermediate.

pHP-GTP is the superior caged compound for the investigation of fast reactions because photolysis is fast and without an intermediate. Indeed, we observe very fast production of GTP from pHP-GTP with only one minor and very fast kinetic rate that might be a heat artifact (Figure S4). For this reason, we use pHP-GTP for the protein reactions shown below.

The protein with its GTPase domain (orange) and all- α domain (yellow) is shown in Figure 3A. The central nucleotide is shown in a ball-and-stick representation. Figure 3B shows the reaction scheme of $G\alpha_i$. After irradiation with a 308 nm excimer laser, we expect the photolysis reaction and subsequently the hydrolysis. The hydrolysis reaction is slow and can be observed by rapid-scan FTIR as a control for our first dual-comb experiments with a protein. In both cases, a global fit of the time-resolved data by applying eq 1 with $n = 1$ describes the data well. This can be recognized for the dual comb experiment by the nice agreement of the time-resolved data at 1215 cm^{-1} with the curve from the fit. Comparing dual comb and FTIR spectra, the amplitude spectra of photolysis a_{ph} and hydrolysis spectra a_1 both agree nicely (Figure 3C,D). The absorption peaks were assigned in the literature by isotopic labeling.^{19,26} In the photolysis, a combined asymmetric stretching vibration of the phosphate groups is assigned, and in the hydrolysis, the asymmetric PO_2 stretching mode of the α -phosphate of GTP is shown. Further, the single-exponential kinetics (Figure 3E) are in line with the literature.¹⁹ After having demonstrated the basic functioning of the dual-comb technique for GTPase reactions of proteins, we want to investigate a very fast reaction, which cannot be observed at room temperature by FTIR. The RGS-catalyzed

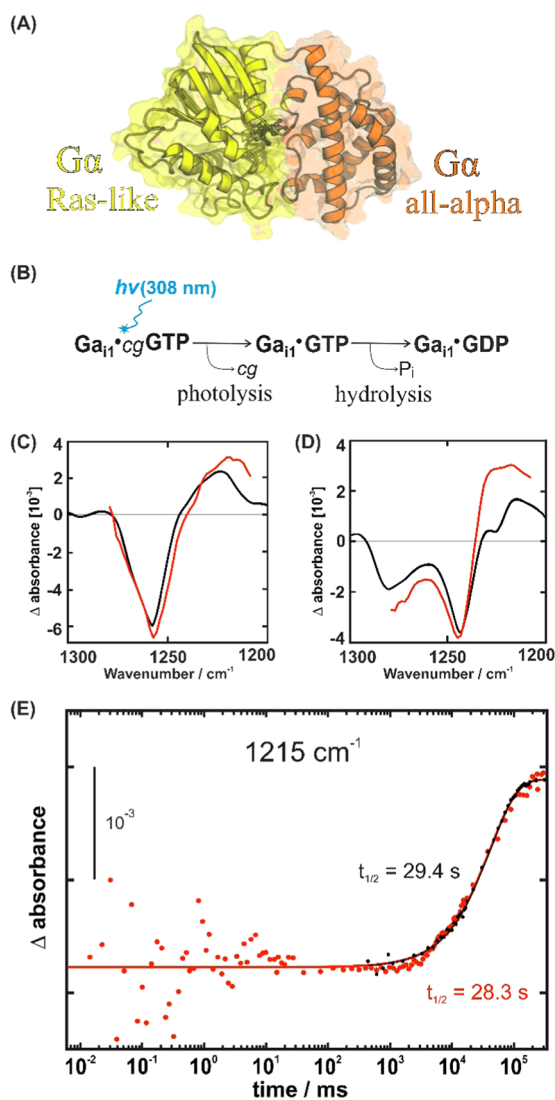


Figure 3. (A) Structural model of $G\alpha_i$ from PDB ID 2G83. (B) Reaction scheme for the GTPase reaction of $G\alpha_i$. (C) Photolysis and (D) hydrolysis spectra obtained by FTIR (black) and dual-comb (red) obtained by global fits of the time-resolved data, respectively. (E) Kinetics of the hydrolysis reaction. The points correspond to the time-resolved data, and the lines correspond to the global fits according to eq 1. The absorption of the dual-comb experiment was normalized to the FTIR experiment, where a thinner sample was used.

reaction of $G\alpha_i$ is much faster than the reaction of $G\alpha_i$ alone and cannot be resolved by rapid-scan FTIR at ambient temperature. The first datapoint in the FTIR measurements of these larger protein–protein complexes (Figure 4A) is usually above 100 ms (see, e.g., Figure 2B in ref 19). With the dual-comb experiment, our first datapoint is at 4 μ s. The kinetics at 1240 cm^{-1} show nicely the decay of the α -GTP band due to the GTPase reaction.¹⁹ Clearly, the reaction is almost complete at 100 ms, indicating that the reaction could not be observed by rapid-scan FTIR at all. A half-life of 90 ms was obtained. Interestingly, there are even two additional very fast rates (Figure 4C half-lives of 38 and 86 μ s) resolved, preceding hydrolysis. We can speculate that one rate corresponds to a heating artifact (as observed for pHP-GTP alone, Figure S3) and the other rate corresponds to a fast rearrangement within the catalytic site. Such a rearrangement was also observed on a slower timescale in a $G\alpha_i$ mutant.²⁷ However, further

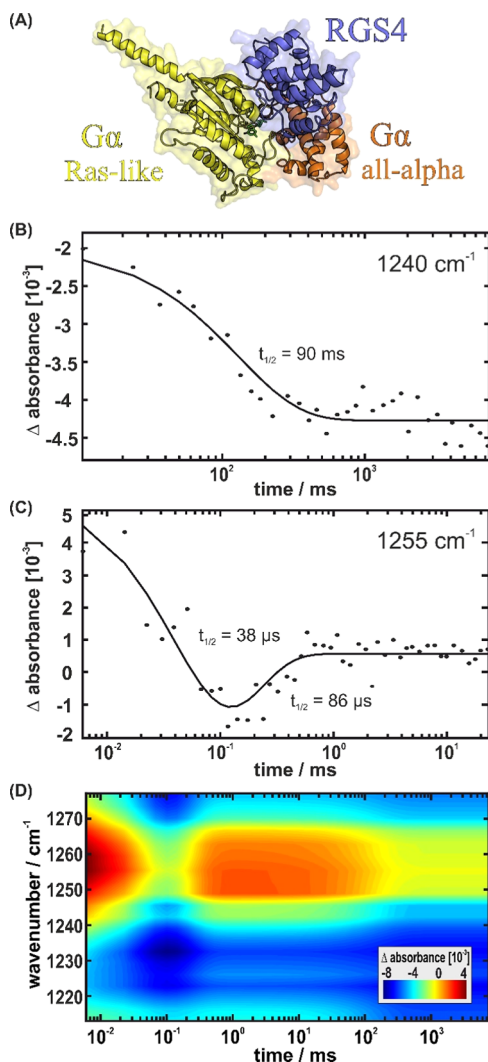


Figure 4. (A) Structural model of $G\alpha_i$ -RGS from PDB ID 1AGR. (B) Kinetics of the hydrolysis reaction of $G\alpha_i$ -RGS. (C) Additional prehydrolysis rates obtained by dual-comb IR. In (B) and (C), the points correspond to the time-resolved data and the line corresponds to the global fit according to eq 1. (D) Three-dimensional (3D) plot of the changes obtained from the global fit (eq 1) of the dual-comb data as detailed in the Experimental Section. After photolysis, three processes ($n = 3$) with half-lives of 38 μ s, 86 μ s, and 90 ms were obtained.

experiments including the measurements of further $G\alpha_i$ mutants will be necessary for a clearcut assignment and is not within the scope of this work. The complete reaction with all of the information obtained in the dual-comb experiment is shown in Figure 4D.

CONCLUSIONS

Overall, we were able to show that the dual-comb setup is very suitable for the investigation of proteins with caged compounds. The only drawback of the new technique is the relatively small spectral window of each dual-comb setup. However, laser modules can be changed and modules for all interesting wavenumbers between 2200 and 900 cm^{-1} are available, and with the about 100 times stronger source power, single-shot analyses of weak absorbers are possible. Another approach could be the measurement of full spectra by FTIR

with low time resolution and subsequent measurement of interesting regions with a dual-comb setup.

We demonstrate that with a single sample, a time resolution in the microsecond regime can be obtained even for a larger protein–protein complex. In our setups, we use a sample thickness of 60 μm , a great advantage of the intense QCLs in comparison to FTIR, where we use about 10 μm sample thickness. This alone should lead to an about 6 times larger S/N ratio. The larger pathlength also allows for a much easier implementation of flow through setups using conventional microfluidics.

■ ASSOCIATED CONTENT

SI Supporting Information

The Supporting Information is available free of charge at <https://pubs.acs.org/doi/10.1021/acs.analchem.1c00666>.

Spectral coverage and intensities of the individual QCL devices (Figure S1); illustration of the acquisition modes of the dual comb spectrometer (Figure S2); photolysis signal development during an experiment (Figure S3); photolysis of pHP-GTP (Figure S4); and comparison of the conventional IR cuvette with the beam diameter of the QCL (Figure S5) (PDF)

■ AUTHOR INFORMATION

Corresponding Author

Carsten Kötting – Competence Center for Biospectroscopy, Center for Protein Diagnostics (ProDi), Ruhr University Bochum, 44801 Bochum, Germany; Department of Biophysics, Faculty of Biology and Biotechnology, Ruhr University Bochum, 44801 Bochum, Germany;
Email: carsten.koetting@rub.de

Authors

Mohamad Javad Norahan – Competence Center for Biospectroscopy, Center for Protein Diagnostics (ProDi), Ruhr University Bochum, 44801 Bochum, Germany; Department of Biophysics, Faculty of Biology and Biotechnology, Ruhr University Bochum, 44801 Bochum, Germany

Raphael Horvath – IRsweep AG, 8712 Staefa, Switzerland

Nathalie Woitzik – Competence Center for Biospectroscopy, Center for Protein Diagnostics (ProDi), Ruhr University Bochum, 44801 Bochum, Germany; Department of Biophysics, Faculty of Biology and Biotechnology, Ruhr University Bochum, 44801 Bochum, Germany

Pierre Jouy – IRsweep AG, 8712 Staefa, Switzerland

Florian Eigenmann – IRsweep AG, 8712 Staefa, Switzerland

Klaus Gerwert – Competence Center for Biospectroscopy, Center for Protein Diagnostics (ProDi), Ruhr University Bochum, 44801 Bochum, Germany; Department of Biophysics, Faculty of Biology and Biotechnology, Ruhr University Bochum, 44801 Bochum, Germany

Complete contact information is available at:

<https://pubs.acs.org/doi/10.1021/acs.analchem.1c00666>

Notes

The authors declare no competing financial interest.

■ ACKNOWLEDGMENTS

The authors thank Dr. Daniel Mann for the preparation of G_{ai} and Dr. Christian Teuber, Adrian Höveler, and Kristin

Labudda for help with the sample preparation. They further thank Dr. Jonas Schartner for the synthesis of pHP-GTP. This work was supported by Deutsche Forschungsgemeinschaft (DFG, German Research Foundation), individual Research Grant GE 599/20-1 to K.G. and KO 3813/1-1 to C.K. and Research Training Group 2341 “MiCon.” Further support was provided by the Ministry for Culture and Science (MKW) of North Rhine-Westphalia (Germany) through grant 111.08.03.05-133974 and the Protein Research Unit Ruhr within Europe (PURE) funded by the Ministry of Innovation, Science and Research (MIWF) of North Rhine-Westphalia (Germany).

■ REFERENCES

- (1) Lorenz-Fonfria, V. A. *Chem. Rev.* **2020**, *120*, 3466–3576.
- (2) Schultz, B.-J.; Mohrmann, H.; Lorenz-Fonfria, V. A.; Heberle, J. *Spectrochim. Acta, Part A* **2018**, *188*, 666–674.
- (3) Rammelsberg, R.; Hessling, B.; Chorogiewski, H.; Gerwert, K. *Appl. Spectrosc.* **1997**, *51*, 558–562.
- (4) Sanchez, M. L. K.; Sommer, C.; Reijerse, E.; Birrell, J. A.; Lubitz, W.; Dyer, R. B. *J. Am. Chem. Soc.* **2019**, *141*, 16064–16070.
- (5) Neumann-Verhoeven, M.-K.; Neumann, K.; Bamann, C.; Radu, I.; Heberle, J.; Bamberg, E.; Wachtveitl, J. *J. Am. Chem. Soc.* **2013**, *135*, 6968–6976.
- (6) Lin, J.; Gerwert, K.; Kötting, C. *Appl. Spectrosc.* **2014**, *68*, 531–535.
- (7) Souvignier, G.; Gerwert, K. *Biophys. J.* **1992**, *63*, 1393–1405.
- (8) Süß, B.; Ringleb, F.; Heberle, J. *Rev. Sci. Instrum.* **2016**, *87*, No. 063113.
- (9) Schade, U.; Ritter, E.; Hegemann, P.; Aziz, E. F.; Hofmann, K. P. *Vib. Spectrosc.* **2014**, *75*, 190–195.
- (10) Ritter, E.; Puskar, L.; Kim, S. Y.; Park, J. H.; Hofmann, K. P.; Bartl, F.; Hegemann, P.; Schade, U. *J. Phys. Chem. Lett.* **2019**, *10*, 7672–7677.
- (11) Klocke, J. L.; Mangold, M.; Allmendinger, P.; Hugi, A.; Geiser, M.; Jouy, P.; Faist, J.; Kottke, T. *Anal. Chem.* **2018**, *90*, 10494–10500.
- (12) Lins, E.; Read, S.; Unni, B.; Rosendahl, S. M.; Burgess, I. J. *Anal. Chem.* **2020**, *92*, 6241–6244.
- (13) Klán, P.; Šolomek, T.; Bochet, C. G.; Blanc, A.; Givens, R.; Rubina, M.; Popik, V.; Kostikov, A.; Wirz, J. *Chem. Rev.* **2013**, *113*, 119–191.
- (14) Barth, A.; Kreutz, W.; Mäntele, W. *FEBS Lett.* **1990**, *277*, 147–150.
- (15) Kötting, C.; Gerwert, K. *Biol. Chem.* **2015**, *396*, 131–144.
- (16) Walker, J. W.; Reid, G. P.; McCray, J. A.; Trentham, D. R. *J. Am. Chem. Soc.* **1988**, *110*, 7170–7177.
- (17) Park, C.-H.; Givens, R. S. *J. Am. Chem. Soc.* **1997**, *119*, 2453–2463.
- (18) Givens, R. S.; Rubina, M.; Wirz, J. *Photochem. Photobiol. Sci.* **2012**, *11*, 472.
- (19) Mann, D.; Teuber, C.; Tennigkeit, S. A.; Schröter, G.; Gerwert, K.; Kötting, C. *Proc. Natl. Acad. Sci. U.S.A.* **2016**, *113*, E8041–E8050.
- (20) Pinkowski, N. H.; Ding, Y.; Strand, C. L.; Hanson, R. K.; Horvath, R.; Geiser, M. *Meas. Sci. Technol.* **2020**, *31*, No. 055501.
- (21) Coddington, I.; Newbury, N.; Swann, W. *Optica* **2016**, *3*, 414.
- (22) Barth, A.; Hauser, K.; Maentele, W.; Corrie, J. E. T.; Trentham, D. R. *J. Am. Chem. Soc.* **1995**, *117*, 10311–10316.
- (23) Cepus, V.; Ulbrich, C.; Allin, C.; Troullier, A.; Gerwert, K. *Methods Enzymol.* **1998**, *291*, 223–245.
- (24) Gerwert, K. Google Patents. WO1999040413A1.
- (25) Rammelsberg, R.; Boudas, S.; Chorogiewski, H.; Gerwert, K. *Vib. Spectrosc.* **1999**, *19*, 143–149.
- (26) Schröter, G.; Mann, D.; Kötting, C.; Gerwert, K. *J. Biol. Chem.* **2015**, *290*, 17085–17095.
- (27) Mann, D.; Höveler, U.; Kötting, C.; Gerwert, K. *Biophys. J.* **2017**, *112*, 66–77.